Breakdown of the Stokes-Einstein relation in two, three and four dimensions

Shiladitya Sengupta[1,2], Smarajit Karmakar[2], Chandan Dasgupta[3], Srikanth Sastry[1,2]

[1] *Theoretical Sciences Unit, Jawaharlal Nehru Centre for Advanced*
Scientific Research, Jakkur Campus, Bangalore 560 064, India.
[2] *TIFR Centre for Interdisciplinary Sciences, 21 Brundavan Colony, Narsingi,Hyderabad 500075, India.*
[3] *Centre for Condensed Matter Theory, Department of Physics,*
Indian Institute of Science, Bangalore, 560012, India.
(Dated: November 6, 2012)

The breakdown of the Stokes-Einstein (SE) relation between diffusivity and viscosity at low temperatures is considered to be one of the hallmarks of glassy dynamics in liquids. Theoretical analyses relate this breakdown with the presence of heterogeneous dynamics, and by extension, with the fragility of glass formers. We perform an investigation of the breakdown of the SE relation in 2, 3 and 4 dimensions, in order to understand these interrelations. Results from simulations of model glass formers show that the degree of the breakdown of the SE relation decreases with increasing spatial dimensionality. The breakdown itself can be rationalized *via* the difference between the activation free energies for diffusivity and viscosity (or relaxation times) in the Adam-Gibbs relation in three and four dimensions. The behavior in two dimensions also can be understood in terms of a generalized Adam-Gibbs relation that is observed in previous work. We calculate various measures of heterogeneity of dynamics and find that the degree of the SE breakdown and measures of heterogeneity of dynamics are generally well correlated but with some exceptions. The two dimensional systems we study show deviations from the pattern of behavior of the three and four dimensional systems both at high and low temperatures. The fragility of the studied liquids is found to increase with spatial dimensionality, contrary to the expectation based on the association of fragility with heterogeneous dynamics.

I. INTRODUCTION

The dramatic slowdown of dynamics upon cooling glass-forming liquids towards the glass transition is described by the temperature dependence of a number of transport coefficients, and relaxation time scales, which include the shear viscosity (η), the translational diffusion coefficient (D), the rotational correlation time (τ_c) and the structural relaxation time τ_α obtained from the long time decay of density correlation functions. The Stokes-Einstein (SE) relation [1–3] in its original formulation relates the translational diffusion coefficient (D) of a macroscopic, or Brownian, probe particle - a single particle property - to the shear viscosity (η) of the liquid - a collective property at a temperature T : $D = \frac{mk_B}{c\pi R}\frac{T}{\eta}$ where m is the mass and R is the radius of the particle, T is the temperature of the liquid and the factor c ($= 6$ or 4) depends on the (stick or slip) boundary condition at the surface of the Brownian particle [1]. Although a hydrodynamic relation, the SE relation is known to be applicable even for the self diffusion of the liquid particles at high temperatures [4]. However, several experiments and simulation studies in the last three decades [5–26, 28–31] have conclusively shown that at low temperatures in supercooled liquids, the SE relation breaks down, such that self diffusion coefficient is much larger than what one may infer, using the SE relation, from the value of the viscosity. Although many works claim that the break down of the SE relation occurs around the mode coupling temperature T_c [27], more recent results (*e.g.* [29]) suggest that the breakdown occurs in the vicinity of a much higher temperature, the onset temperature T_{onset}, at which as-

pects of slow dynamics including stretched exponential relaxation (see below) begin to be manifested [32–34]. There is a commonly held view that the breakdown of the SE relation is a manifestation of dynamical heterogeneity (DH), which is characterized by various indicators we discuss below, such as the dynamical susceptibility (χ_4)[35–40], the Kohlrausch-William-Watts (KWW) exponent (β_{KWW}) quantifying the stretched exponential decay of correlation functions, and the non-Gaussian parameter α_2 that measures the deviation of particle displacements from a Gaussian form. We note, however, that there is no agreement on the nature and origin of heterogeneity among the theories proposed to explain the SE breakdown (*e.g.*, dynamical facilitation [41], the random first order transition theory [42–44], the mode-coupling theory [45], the shear transformation zone theory [46] and the obstruction model [47]). The goal of the present work is to interrogate the manner in which the SE breakdown changes with the spatial dimensionality, and the correlation of SE breakdown with characteristics of heterogeneous dynamics, and fragility. Since the spatial dimensionality enters explicitly in some of the theoretical descriptions mentioned above, this study is expected to provide valuable information about the validity of these theories. As we discuss below, our investigations reveal surprises whose rationalization should lead to a better understanding of the key features of glassy dynamics.

The rest of this paper is organized as follows: In Sec. II, we provide a discussion of the SE relation and its relation with dynamical heterogeneity and fragility, that forms the necessary background for our work. In Sec. III we provide details regarding the models studied and the simulation procedure. Sec. IV contains the results of

our study. Sec. V contains a discussion and conclusions arising from our work.

II. STOKES-EINSTEIN BREAKDOWN, DYNAMICAL HETEROGENEITY AND FRAGILITY

One of the earliest theories of the breakdown of the SE relation is due to Hodgdon and Stillinger [4] who envisage the highly viscous supercooled liquid to be composed of sparse "fluid-like" regions of low viscosity in a matrix of a more viscous fluid. Thus, both D and η are space-dependent. By calculating the viscous drag force on a diffusing particle in the "fluid-like" region, they showed that the local drag force decreases from the Stokes' value, and hence the local diffusion coefficient increases. If one uses the bulk viscosity (which is dominated by the more viscous regions) in the SE relation, one finds a breakdown of this relation. In order to apply their model to realistic systems and to explain the difference between the behavior of translational and rotational diffusion coefficients, Hodgdon and Stillinger had to impose certain special properties on their model. However, Tarjus and Kivelson [17] later argued that the mere existence of domains with different local properties is a sufficient condition for the SE breakdown. They considered a liquid in which there are domains (of unspecified nature) of size L with a size distribution $\rho(L)$ such that $\rho(L)L^2dL$ is the probability of finding a molecule in a domain of size between L and $L + dL$. They assumed that the local relaxation time $\tau(L)$ in a domain is size dependent and the measured α relaxation time (τ_α) is the average of $\tau(L)$:

$$
\begin{aligned}
\tau_L &\propto \exp(E(L)/k_BT) \\
\tau_\alpha = \langle \tau_L \rangle &\propto \int_0^\infty \rho(L) \exp(E(L)/k_BT)L^2dL \quad (1)
\end{aligned}
$$

In their picture, the SE relation is valid inside a domain. However, the translational diffusion involves passage through many domains. This is why the average D is different from the prediction of the SE relation. Assuming that a diffusing particle performs a random walk across domains and $D(L)$ changes abruptly at interfaces, and neglecting a term involving the gradient of D, one obtains:

$$
\begin{aligned}
D(L) &\propto T/\eta(L), \quad \eta(L) \propto \exp(E(L)/k_BT) \\
D = \langle D(L) \rangle &\propto \int_0^\infty \rho(L)D(L)L^2dL \\
&\propto \int_0^\infty \rho(L) \exp(-E(L)/k_BT)L^2dL \quad (2)
\end{aligned}
$$

Unless $\rho(L)$ is a δ-function, Eqs. 1 and 2 lead to a violation of the normal behaviour, $D\tau = constant$.

This picture of the heterogeneity may also be interpreted in terms of the existence of a distribution of local relaxation times. Blackburn et al. [10] argued that the translational diffusion coefficient D and the rotational correlation time τ_c measure different moments of this distribution, thus causing the SE breakdown:

$$
\begin{aligned}
D &\propto \langle \frac{1}{\tau} \rangle, \quad \tau_c = \langle \tau \rangle \\
D\tau_c &\propto \langle \tau \rangle \langle \frac{1}{\tau} \rangle
\end{aligned}
$$

$$
\langle \tau \rangle \langle \frac{1}{\tau} \rangle = \begin{cases} 1 \text{ for } \delta \text{ function distribution, normal SE} \\ \quad > 1 \text{ SE breakdown} \end{cases}
$$
(3)

La Nave et al. showed, [48] using the potential energy landscape framework, that in the 3D Kob-Andersen model [49] the product $< D >< 1/D >$ indeed grows as the temperature decreases. Swallen et al. [12] argued that since $D\tau_c$ increases with decreasing temperature, Eq. 3 implies that the distribution of relaxation time should be broader at lower T.

The stretching exponent β_{KWW} provides a measure of the width of the distribution of relaxation times. Let $\rho(\tau)$ denote the distribution of relaxation times τ where each of the local relaxation function is exponential with relaxation time τ. The overall correlation function $\phi(t)$ is empirically given by a stretched exponential:

$$
\phi(t) = \int_0^\infty d\tau \rho(\tau) \exp(-t/\tau) = \exp\left(-(t/\tau_{KWW})^{\beta_{KWW}}\right)
$$

Using simple mathematical identities, it can be shown [50] that the n-th moment $\langle \tau^n \rangle$ of the distribution $\rho(\tau)$ is given by

$$
\langle \tau^n \rangle = \frac{\tau_{KWW}^n}{\beta_{KWW}} \frac{\Gamma\left(\frac{n}{\beta_{KWW}}\right)}{\Gamma(n)}
$$
(4)

Using the above formula, it is easy to show that the relative variance, which provides a measure of the width of the distribution, is given by:

$$
\frac{\langle \tau^2 \rangle - \langle \tau \rangle^2}{\langle \tau \rangle^2} = \frac{\beta_{KWW}\Gamma\left(\frac{2}{\beta_{KWW}}\right)}{\Gamma\left(\frac{1}{\beta_{KWW}}\right)} - \Gamma\left(\frac{1}{\beta_{KWW}}\right)
$$
(5)

This equation implies that the relative variance depends *only* on β_{KWW} and increases monotonically as β_{KWW} decreases.

The above analysis suggests the following interpretation of the SE breakdown. As the temperature decreases, DH (of unspecified nature) develops which leads to the existence of a distribution of local relaxation times, the width of which increases as T is decreased. This is manifested as (i) the lowering of β_{KWW} and (ii) the SE breakdown. Since both the SE breakdown and the lowering of β_{KWW} from 1 are manifestations of DH, they should occur simultaneously according to this interpretation.

We should, however, note the following points that argue against this interpretation: (i) the lowering of β_{KWW} does not *prove* the existence of a distribution of relaxation times [50] *i.e.* liquids at low temperatures can be dynamically homogeneous with a single relaxation time but exhibit an inherently non-exponential decay of correlation functions and (ii) some experiments on OTP seem to suggest that β_{KWW} remains *constant* in the relevant low-temperature range (See [12] and references therein). In that case the width of the distribution does not change with temperature, and Eq. 3 can not explain the observation that the degree of the SE breakdown becomes progressively larger as the temperature is decreased.

The DH can be quantified by more direct indicators. In the present study, we have used the following quantities to characterize the DH.

a. The dynamical susceptibility χ_4: The dynamical susceptibility $\chi_4(t)$, which is the integral of the four-point correlation function $g_4(\vec{r}, t)$, measures the *fluctuation* in the two-point correlation function $q(t)$ (overlap function) [39]. Thus $\chi_4(t)$ is a direct measure of the DH. For supercooled liquids, $\chi_4(t)$ shows a peak at a time proportional to the α relaxation time [39]. The peak value of the dynamical susceptibility - χ_4^{peak} - is a direct measure of the volume of space correlated during structural relaxation [40]. Experiments and simulations, typically carried out in three dimensions, show that $\chi_4^{\text{peak}}(T)$ grows monotonically as the temperature T is lowered, which indicates that larger regions of space are dynamically correlated at lower temperature *i.e.* the DH is more prominent at lower temperature.

b. The stretching exponent β_{KWW}: The stretching exponent β_{KWW} is a measure of how non-exponential the decay of a time correlation function is. According to the interpretation of the non-exponential decay of the density-correlation function as a manifestation of heterogeneous dynamics, a lower value of β_{KWW} implies stronger DH.

c. The non-Gaussian parameter $\alpha_2(t)$: This parameter quantifies the deviation of the distribution of particle displacements in time t from the Gaussian form expected for spatially homogeneous dynamics. The non-Gaussian parameter, calculated from the second and fourth moments of the distribution of the displacements, exhibits a peak at a characteristic time that increases as the temperature is decreased. The peak value of α_2 provides a characterization of the spatial heterogeneity of the dynamics.

d. Fragility: Fragility is a material parameter that measures how rapidly the viscosity (or relaxation time) of supercooled liquids increases as the temperature decreases. Böhmer *et al.* [51] in their extensive compilation of available data found that the kinetic fragility m determined from the slope of the Angell plot at T_g has negative correlation with the stretching exponent β_{KWW}, *i.e.*, smaller β_{KWW} implies a higher fragility. This conclusion remains the same for both isobaric and isochoric

fragilities [52]. Such a relation has also been obtained theoretically within the framework of random first order transition theory [43]. Based on this correlation between fragility and β_{KWW}, fragility can be considered to be an indicator of DH - *more fragile systems are more heterogeneous.*

However, there are evidences against this correlation as well: (i) In experiments on supercooled water confined in nano-pores, Chen *et al.* [22] observed a fragile to strong transition and found fractional SE relations in both the regimes. However, the breakdown exponent is closer to 1 (= 0.74) for fragile water than that for strong water (= 0.67). (ii) Similarly, the breakdown exponent *computed* by Jung *et al.* [41] using dynamical facilitation theory was also closer to 1 (= 0.73) for a fragile glass-former model than for a strong glass-former model (= 0.67). (iii) In [53] it was shown that the strong correlation found by Böhmer *et al.* [51] between the kinetic fragility and β_{KWW} becomes much weaker if subgroups (*e.g. only* simple or complex molecular glass-formers) are considered. (iv) Dyre also claimed [54], on the basis of experiments on simple, organic glass-forming liquids that no clear correlation is present between these two quantities. (v) In the simulation of ST2 water, Becker *et al.* [23] observed a breakdown of the SE relation at low T in both strong and fragile regimes, with the breakdown exponent nearly the same for both strong and fragile water. (vi) Vasisht and Sastry [55], similarly find in simulations of silicon that the SE breakdown becomes apparent in the high temperature, high density liquid, and the breakdown exponent is the same in both the high temperature (fragile) and low temperature (strong) liquids.

We emphasize, however, that the above picture is based on experiments and simulations predominantly in three dimensions and does not, *a priori*, tell us what to expect in other spatial dimensions. In the present study, we aim to understand the inter-relations among DH, the SE breakdown and the fragility in other spatial dimensions by studying model glass-forming liquids in 2, 3 and 4 dimensions and by considering *both* the SE breakdown and direct measures (χ_4, β_{KWW}, α_2) of DH and fragility.

We end this section by remarking on the study of SE relation in two dimensions. Strictly speaking, transport coefficients such as η and D are not well-defined in infinitely large two-dimensional systems at equilibrium due to the presence of long-time tails [56, 57] in correlation functions appearing in the Green-Kubo formulae for these transport coefficients, and for similar reasons the the use of the Stokes relation is questionable [58]. However, these effects are not important for the length and time scales considered in our 2D simulations. We find well-defined diffusive behavior (mean-square displacement proportional to time) at long times in all our 2D simulations, from which the diffusion coefficient D can be obtained without any ambiguity. This is consistent with the results of several existing MD simulations of 2D model systems [59–62] in which the diffusion coefficient and the viscosity have been computed and the

validity of the SE relation has been examined [60].

III. SIMULATION DETAILS

In the present study we perform NVT MD simulations for the following models : (a) the Kob-Andersen binary mixture at the canonical $80 : 20$ composition [49] in 4, 3 and 2 dimensions (denoted by 4D KA, 3D KA, 2D KA respectively) at number densities $\rho = 1.60$ (4D), $\rho = 1.20$ (3D and 2D); (b) the modified Kob-Andersen model (denoted by 2D MKA) at a different composition $65 : 35$ [63] at the number density $\rho = 1.20$; (c) the 50:50 binary mixture of purely repulsive soft spheres with potential $V(r) \sim r^{-10}$ in 3 and 2 dimensions (denoted by 3D R10 and 2D R10 respectively) at a number density $\rho = 0.85$ [64]. The details of the potentials and units are described in the corresponding references. The integration time step was in the range $dt \in [0.001 - 0.006]$ depending on the temperature. An algorithm due to Brown and Clarke [65] was used to keep the temperatures constant. System sizes were (1) $N = 1500$ for 4D KA; (2) $N = 1000$ for 3D KA; (3) $N = 1000$ for 2D KA; (4) $N = 2000$ for 2D MKA; (5) $N = 10000$ for 3D R10 and (6) $N = 2048$ for 2D R10. Runlengths at each temperature were at least $100\tau_\alpha$ (the α relaxation time defined below).

We have computed the following measures of time scales :

1. Translational diffusion coefficients D_A of one type of particles measured from the mean squared displacement (MSD) of that type of particles.

2. α relaxation times estimated from the time taken to decay to $1/e$ of the initial value of (a) the overlap function $q(t)$ [36–39, 66], (b) the intermediate scattering function $F(k, t)$, and (c) the self part of the intermediate scattering function $F_{sA}(k, t)$ for one type of particles. The value of k corresponds to the first peak of the partial structure factor $S_{AA}(k)$ of one type of particles.

   Our procedure for computing the overlap function is defined in [67]. The intermediate scattering function $F(k, t)$ and its self part $F_s(k, t)$ are defined as

$$F(\vec{k}, t) = \sum_{i=1}^{N} \sum_{j=1}^{N} e^{-i\vec{k}\cdot(\vec{r}_i(t) - \vec{r}_j(0))}$$

$$F_s(\vec{k}, t) = \sum_{i=1}^{N} e^{-i\vec{k}\cdot(\vec{r}_i(t) - \vec{r}_i(0))}$$

$$(6)$$

3. The shear viscosity (η) computed from equilibrium simulations using the Einstein and the Green-Kubo relations. The Green-Kubo relation for the shear viscosity is given by the integral of the auto correlation function of the stress tensor $P_{\alpha\beta}(t)$:

$$\eta = \frac{V}{k_B T} \int_0^\infty dt < P_{\alpha\beta}(t) P_{\alpha\beta}(0) >$$

$$P_{\alpha\beta}(t) = \frac{1}{V} \left(\sum_{i=1}^{N} p_{i\alpha} p_{i\beta}/m + \sum_{i=1}^{N} \sum_{j>i}^{N} r_{ij\alpha} f_{ij\beta} \right) \quad (7)$$

where $r_{ij} = |\vec{r}_i - \vec{r}_j|$ and $f_{ij} = -\frac{\partial U(r_{ij})}{\partial r_{ij}}$ and $\alpha, \beta \in (x, y, z)$ denotes Cartesian components.

The shear viscosity can also be computed from the corresponding Einstein relation as the slope of the Helfand moment at long time and in linear regime :

$$\eta = \frac{1}{V k_B T} \lim_{t \to \infty} \frac{< (A_{\alpha\beta}(t) - A_{\alpha\beta}(0))^2 >}{2t} \quad (8)$$

where $A_{\alpha\beta}(t)$ is the Helfand moment and related to the stress tensor as

$$\frac{dA_{\alpha\beta}(t)}{dt} = P_{\alpha\beta}(t) V$$

Since the shear viscosity is a collective property of N particles, numerical accuracy is a big issue when computing shear viscosity using either Eq. 7 or Eq. 8. To improve numerical accuracy we take average over different components. We have found that values from the two methods mutually agree well and report here the shear viscosity obtained from the Einstein method (denoted by $\eta_{Einstein}$).

IV. RESULTS

In this section, we describe our results for the SE breakdown, fragility and different measures of DH in 2, 3 and 4 dimensions. In Sec. IV (A) we show diffusivity, viscosity and relaxation time data that demonstrate the SE breakdown. We further show that in 3 and 4 dimensions, the breakdown exponent can be understood in terms of the Adam-Gibbs relation for diffusivity and relaxation time. In 2 dimensions, the Adam-Gibbs relation is not valid as we have previously shown [68]. We show here that nevertheless, the the SE breakdown in two dimensional systems can be rationalized in terms of a generalized Adam-Gibbs relation observed to hold in these systems. In Sec. IV (B) we describe various measures by which heterogeneity can be quantified, and the correspondence of the degree of heterogeneity with the degree of the SE breakdown. In Sec. IV (C) we show that fragility increases with increasing spatial dimensionality, contrary to expectations that the fragility is correlated with the degree of heterogeneity of dynamics. We show however that the variation of fragility with dimensionality can be understood in thermodynamic terms, through the evaluation of the configurational entropy and properties of the distribution of local energy minima or inherent structures [69].

A. The dimension dependence of the SE breakdown

The breakdown of the SE relation in three dimensions in the Kob-Andersen model has been reported earlier [15, 29, 30]. Our data agree reasonably well with those of previous studies. Here we study the dependence of the SE relation on the spatial dimension by considering the following models which are defined in the previous section: (i) 2DKA, (ii) 2DMKA (iii) 2DR10, (iv) 3DKA and (v) 4DKA. According to the SE relation, the quantity $D\eta/T$ should be independent of the temperature T – deviations of this ratio from a constant value as the temperature is changed would constitute a violation of the SE relation. Since the viscosity η is difficult to calculate in a molecular dynamics simulation, the temperature dependence of $D\tau_\alpha$ or $D\tau_\alpha/T$ has been considered in most existing numerical studies to investigate the validity of the SE relation. These choices correspond to a replacement of η by τ_α assuming either that $\tau_\alpha \propto \eta$ or $\tau_\alpha \propto \eta/T$. The justification for these substitutions obtain from either the Maxwell relation ($\eta = G_\infty \tau$) or the relationship between relaxation times and the diffusion coefficient in the diffusive regime ($\tau^{-1} = Dq^2 = \frac{mk_Bq^2}{c\pi R}\frac{T}{\eta}$; this argument assumes the validity of the SE relation). From various experimental and simulation results, [70–72], $\tau_\alpha \propto \eta/T$. Consistently with previous observations, we find that $\tau_\alpha \propto \eta/T$ provides a very good description of the low-temperature data over a fairly large range of η and τ_α, as shown in Fig.1, using viscosities calculated from the Green-Kubo formula and the Einstein relation for the 3DKA model. We therefore use the following two representations to analyze the degree of SE violation from the data.

i In a D_A vs. τ_α or $\frac{\eta}{T}$ plot (D_A is the calculated diffusion coefficient of particles of type A), by fitting the data to a power law of the form $D_A \propto \tau_\alpha^{-\xi}$, or $D_A \propto \left(\frac{\eta}{T}\right)^{-\xi}$ we test if the effective exponent ξ is different from unity, the prediction of the SE relation.

ii From the T dependence of $D_A\tau_\alpha$ or $\frac{D_A\eta}{T}$, we test if these quantities are constant (SE relation obeyed) or become T dependent (breakdown of the SE relation).

The breakdown of the SE relation in 2, 3 and 4 dimensions is shown in Figs. 2 (2DKA), 3 (2DMKA), 4 (2DR10), 5(3DKA), 6(3DR10) and 7 (4DKA). In most of the cases (excepting 2DKA and 3DR10) we show data ranging from high temperatures, well above the onset temperature T_{onset}, to well below T_{onset}. A change from Arrhenius to super-Arrhenius temperature dependence of relaxation times defines the onset temperature of slow dynamics [32–34] T_{onset}. The onset temperature is close in all cases to the temperature at which one observes the breakdown of the SE relation, T_{SEB} as described below. All the simulations reported here are performed at temperatures above the mode coupling temperatures T_c for
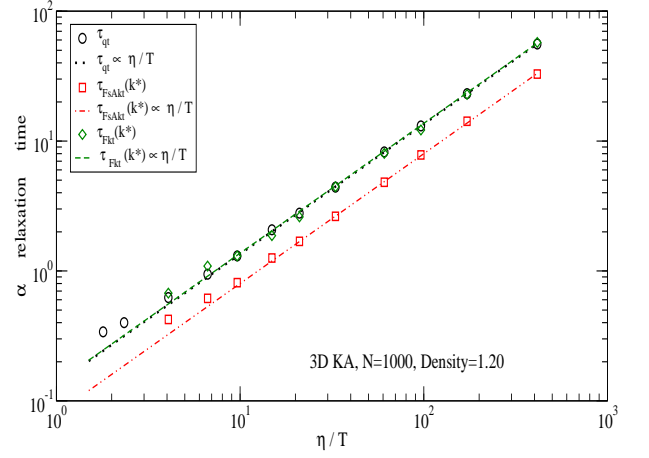

FIG. 1: α relaxation times τ obtained from (i) the overlap function (τ_{qt}, (ii) the self part (τ_{FsAkt}) of the intermediate scattering function $F_{sA}(k^*, t)$ of one type (A) of particles and (iii) from the full (τ_{Fkt}) intermediate scattering function $F(k^*, t)$ plotted against viscosity showing that $\tau \propto \eta/T$ is a good description of data at low T in the 3D KA model. Systematic deviations are seen at high T. k^* is at the first peak of the partial structure facture $S_{AA}(k)$.

the respective models, and the T_{SEB} we obtain are well above the T_c values.

one below the other in single column instead of messing with two column figures.

From the D_A vs. τ_α or $\frac{\eta}{T}$ plots, we see that in *all* spatial dimensions, the low T data follow a fractional power-law relation, indicating a breakdown of the SE relation. For the same model (KA) in different dimensions the power-law exponent ξ is closer to 1 in higher dimensions, indicating that the SE breakdown is weaker in higher dimensions [73, 74]. The difference in the exponent in two and three dimensions however is very small and essentially negligible. Similarly for the R10 model, the exponent is marginally, but negligibly, higher in three dimensions. The MKA model in two dimensions has an exponent that is very close to the KA model in the same dimension. All the model results taken together, the breakdown exponent is different for different models in the same dimension.

Further, as the temperature increases, there is a clear change of the exponent value in D_A vs. τ_α or $\frac{\eta}{T}$, plots indicating a *qualitative* difference between high T and low T behaviours. Surprisingly, in two dimensions, in both the models for which high T data are shown (2DMKA and 2DR10), the high T exponent from D_A vs. τ_α plots is *higher than 1*. However, in 3 dimensions, the SE relation $D_A \propto \frac{\eta}{T}$ is recovered at high T as expected. Finally, as we go to still higher dimension ($D = 4$), the D_A vs. τ_α plot shows the expected relation ($D_A \propto \tau_\alpha^{-1}$) at high T.

The above correlation between D_A and τ_α is also reflected in the T dependence of $D_A\tau_\alpha$. Since the diffusion coefficient decreases but the relaxation time in-

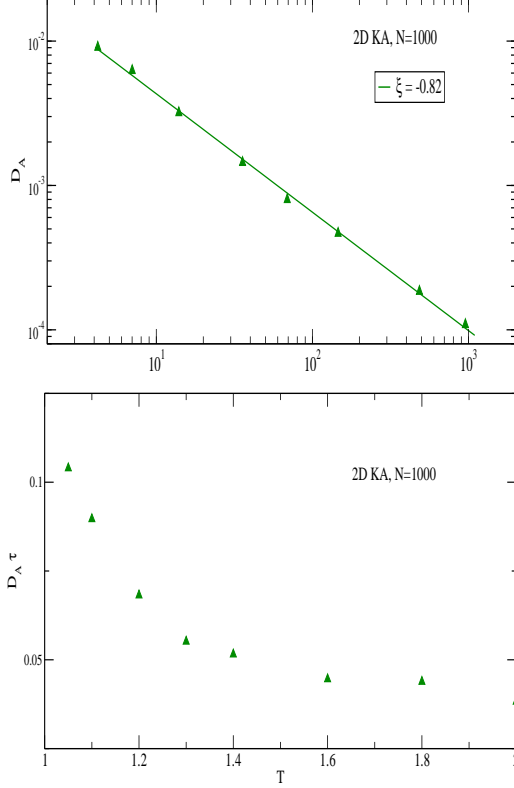FIG. 2: Plot showing the breakdown of the SE relation in the 2D KA model at low temperatures. *Top*: D_A *vs.* τ plot (Here τ is the α relaxation time from the overlap function $q(t)$). *Bottom*: T dependence of $D_A\tau$. The data shown follow a fractional SE relation.

creases as the temperature decreases, there is a competition between two opposing effects. The respective rates of increase and decrease with T exactly cancel each other *only* if the exponent is 1. Since in 2D, the exponent is never 1, the quantity $D_A\tau_\alpha$ goes through a minimum and approaches a constant value only at very high temperatures. In 3D and 4D, $D_A\tau_\alpha$ becomes constant at high T as expected and it *increases* as T decreases at low T, indicating a breakdown of the SE relation.

We have also considered the behaviour of D_A/T *vs.* τ_α and the T dependence of $\frac{D_A\tau_\alpha}{T}$. This corresponds to assuming that $\tau_\alpha \propto \eta$. The D_A/T *vs.* τ_α plots show a fractional SE relation at low T in *all dimensions*. The values of the breakdown exponents from the D_A/T *vs.* τ_α plot are slightly different from those obtained from the D_A *vs.* τ_α plots. However, they show the same trend: the magnitude of the exponent is closer to 1 at higher dimensions, indicating that the SE breakdown is weaker at higher dimensions. The estimates of the breakdown exponents are summarized in Table I.

TABLE I: Estimates of the magnitude of the SE breakdown exponents in different spatial dimensions D. *Notations:* (a) ξ^{SE} = SE breakdown exponent obtained from D_A *vs.* τ_α or $\frac{\eta}{T}$ plots; (b) ξ^{AG} = ratio of slopes from AG plots using D_A and τ_α; High T exponents are obtained from D_A *vs.* τ_α plots.

D	Model	Low T Exponents		High T exponents
		ξ^{SE}	ξ^{AG}	
2	2DR10	0.75	-	1.18
2	2DKA	0.82	-	-
2	2DMKA	0.84	-	1.50
3	3DR10	0.752	-	-
3	3DKA	0.83	0.85	≈ 1
4	4DKA	0.90	0.90	$0.98 \approx 1$

Figs. 3, 4, 5 and 7 also show that the temperature of SE breakdown (T_{SEB}), estimated as the point of interaction of the low T and the high T fits in D_A *vs.* τ_α or $\frac{\eta}{T}$ plots, is close to the Arrhenius to non-Arrhenius cross-over temperature T_{onset} in all dimensions. Thus, the SE breakdown occurs at a temperature that is much higher than the divergence temperature T_c of the mode-coupling theory estimated from a power-law fit of the T-dependence of the relaxation time.

The fractional SE behaviour at low T can be rationalized by considering the *different* dependence of the diffusion coefficient and the α relaxation time on the configuration entropy (S_c). The Adam-Gibbs (AG) relation $X = X_0 \exp(\frac{A_x}{TS_c})$, if it is valid, provides a way to test this hypothesis quantitatively (X is τ_α or $(D_A)^{-1}$ in the present study). Fig. 8 shows that the AG relation is valid in the 3DKA model (top row) and the 4DKA model (bottom row). We see that the slope of the $(D_A)^{-1}$ *vs.* $(TS_c)^{-1}$ plot is *different* from that of the τ_α *vs.* $(TS_c)^{-1}$ plot. Table I shows that the observed fractional SE exponent at low T can be interpreted as the ratio of the slopes in the AG plots in Fig. 8.

In the two dimensional models one sees a deviation from the AG relation at low temperatures. But the behaviour can still be rationalized by considering the generalized Adam-Gibbs relation that is a good description of the data [68]. Thus, we can write

$$\ln D_A = \ln D_0 - \left(\frac{A_D}{TS_c}\right)^{\alpha_D}$$

$$\ln \tau = \ln \tau_0 + \left(\frac{A_\tau}{TS_c}\right)^{\alpha_\tau}$$

$$\ln D_A = \ln D_0 - \left(\frac{A_D}{A_\tau}\right)^{\alpha_D} \left[\ln \frac{\tau}{\tau_0}\right]^r$$

$$r \equiv \frac{\alpha_D}{\alpha_\tau} \tag{9}$$

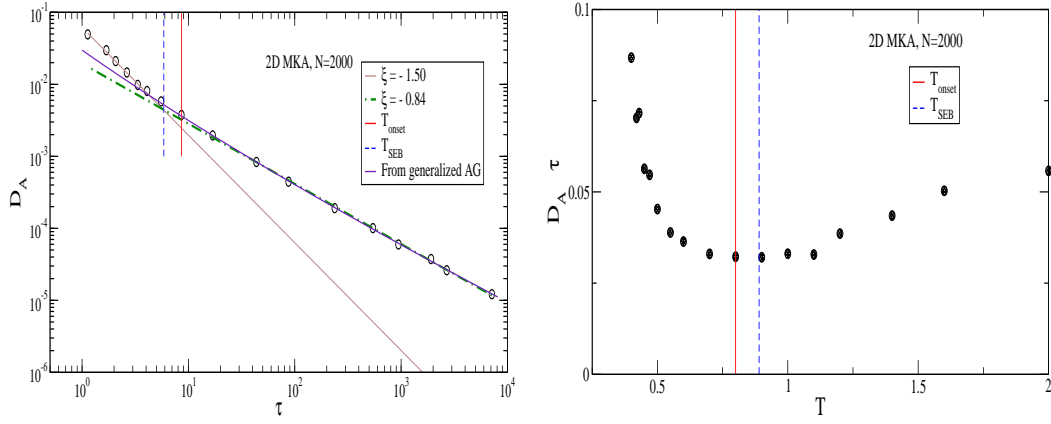Eq. 9 provides the relationship between D and τ based on each obeying a generalized Adam-Gibbs rela-

FIG. 3: Plots showing the breakdown of the SE relation in the 2DMKA model. *Left*: D_A *vs.* τ plot (Here τ is the α relaxation time from the overlap function $q(t)$). *Right:* T dependence of $D_A\tau$. The low T data follow a fractional SE relation. A clear change of exponent occurs at high T in D_A *vs.* τ plot, although *the high T exponent is bigger than 1.* The change of slope occurs at a temperature T_{SEB} which is close to T_{onset}. (T_{SEB} estimated as the point of intersection of high T and low T fits; T_{onset} is the onset temperature of slow dynamics.) Also shown is the dependence of D on τ according to the generalized Adam-Gibbs relation discussed in the text.

FIG. 4: Plots showing the breakdown of the SE relation in the 2DR10 model. *Left*: D_A *vs.* τ plot (Here τ is the α relaxation time from the overlap function $q(t)$). *Right:* T dependence of $D_A\tau$. The low T data follow a fractional SE relation. A clear change of exponent occurs at high T in D_A *vs.* τ plot, although *the high T exponent is bigger than 1.* The change of slope occurs at a temperature T_{SEB} which is close to T_{onset}. (T_{SEB} estimated as the point of intersection of high T and low T fits; T_{onset} is the onset temperature of slow dynamics.) Also shown is the dependence of D on τ according to the generalized Adam-Gibbs relation discussed in the text.

tion, which are shows for 2DMKA and 2DR10 models in Figs. 3, 4. It is seen that indeed the low temperature data as well as some part of the high temperature data are well described by this form. It must be noted that the Eq. 9 is *not* a fractional SE relation, and thus, the description of the data for these two dimensional systems through a breakdown exponent is an approximation.

To summarize, results presented here show that: (i) the SE breakdown in weaker in four dimensions than in three dimensions which is consistent with earlier works [73, 74]. (ii) The breakdown exponent can be rationalized from the different scaling of the diffusion coefficient and the relaxation time with the configurational entropy,

either via the AG relation (three and four dimensions) or a generalized AG relation (two dimensions). (iii) The behaviour in two dimensions is more complicated, displaying no temperature regime where the SE relation is valid, consistently with earlier work [75]. (iv) The SE breakdown temperature T_{SEB} is, in all cases, very close to the onset temperature T_{onset}.
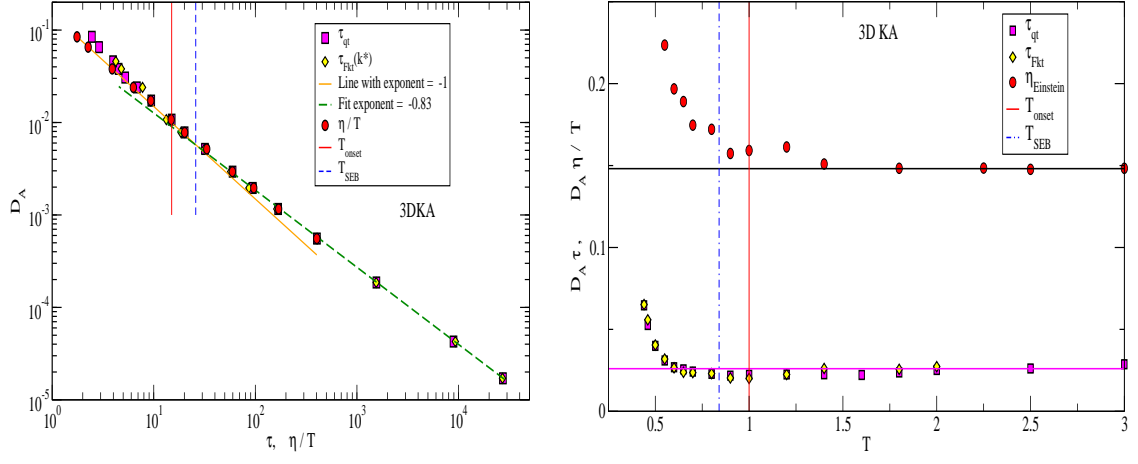
FIG. 5: Plots showing the breakdown of the SE relation in the 3DKA model. The α relaxation times τ are computed from the (i) overlap function (τ_{qt}) (ii) $F(k,t)$ at the peak of $S(k)$ (τ_{Fkt}) These two measures are mutually proportional and are used interchangeably. *Left:* D_A *vs.* τ and $\frac{\eta}{T}$ plot. τ_{qt}, $\tau_{Fkt}(k^*)$ are multiplied by constant factors to match all data sets at low temperature. *Right:* T dependence of $D_A\tau$ and $\frac{D_A\eta}{T}$. The low T data follow a fractional SE relation. A clear change of exponent occurs at high T in the D_A *vs.* τ plot. The high T exponent (=-1) expected from the SE relation is obtained from the D_A *vs.* $\frac{\eta}{T}$ plot. The SE breakdown occurs at a temperature T_{SEB} closer to the onset temperature T_{onset} than T_c [16]. (T_{SEB} estimated as the point of intersection of high T and low T fits; T_{onset} is the Arrhenius to non-Arrhenius cross-over temperature; T_c is the mode coupling transition temperature. All data points shown here are at $T > T_c$.)
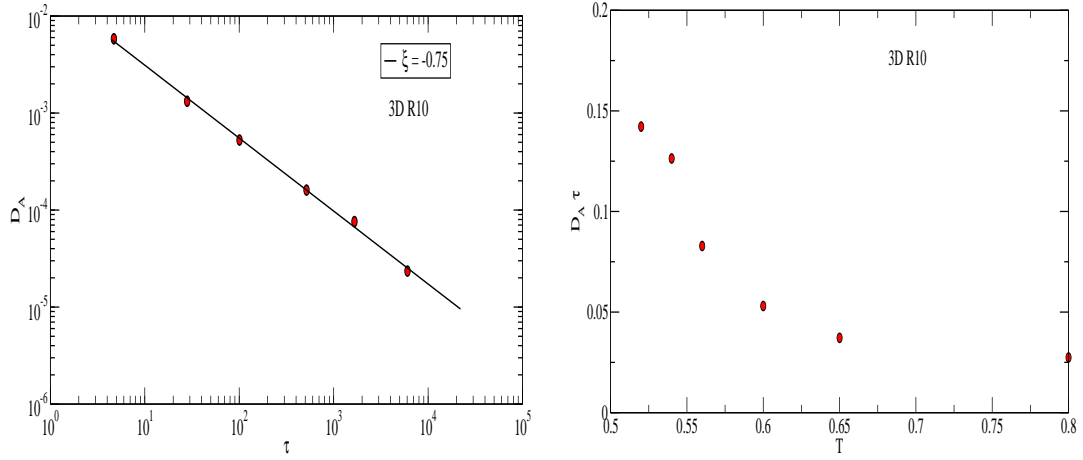
FIG. 6: Plot showing the breakdown of the SE relation in the 3D R10 model at low temperatures. *Left:* D_A *vs.* τ plot (Here τ is the α relaxation time from the overlap function $q(t)$). *Right:* T dependence of $D_A\tau$. The data shown follow a fractional SE relation.
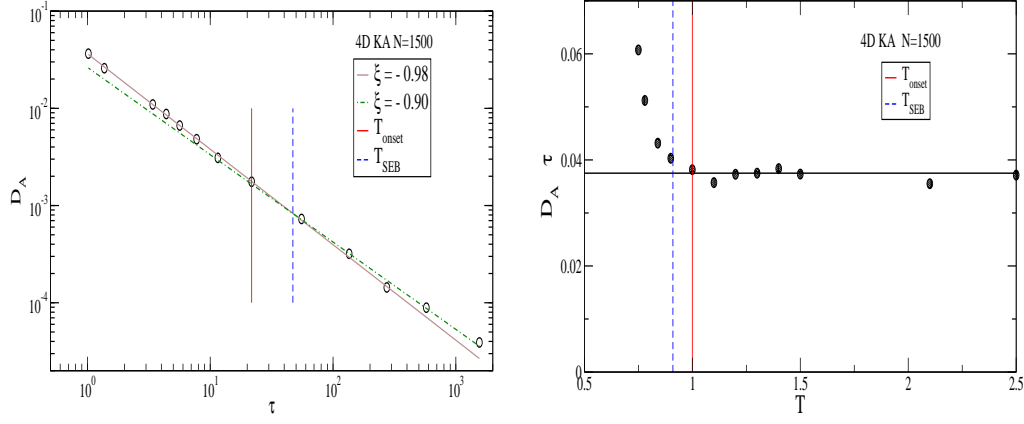
FIG. 7: Plots showing the breakdown of the SE relation in the 4DKA model. *Left*: D_A *vs.* τ plot (τ here is the α relaxation time from the overlap function $q(t)$). *Right:* T dependence of $D_A\tau$. The low T data follow a fractional SE relation. A clear change of exponent occurs at high T in D_A *vs.* τ plot. The high T exponent (=-1) expected for a homogeneous (Gaussian distribution of particle displacements) system is obtained from D_A *vs.* τ plot. The SE breakdown occurs at a temperature T_{SEB} closer to the onset temperature T_{onset} than T_c. (T_{SEB} estimated as the point of intersection of high T and low T fits; T_{onset} is the Arrhenius to non-Arrhenius cross-over temperature.)
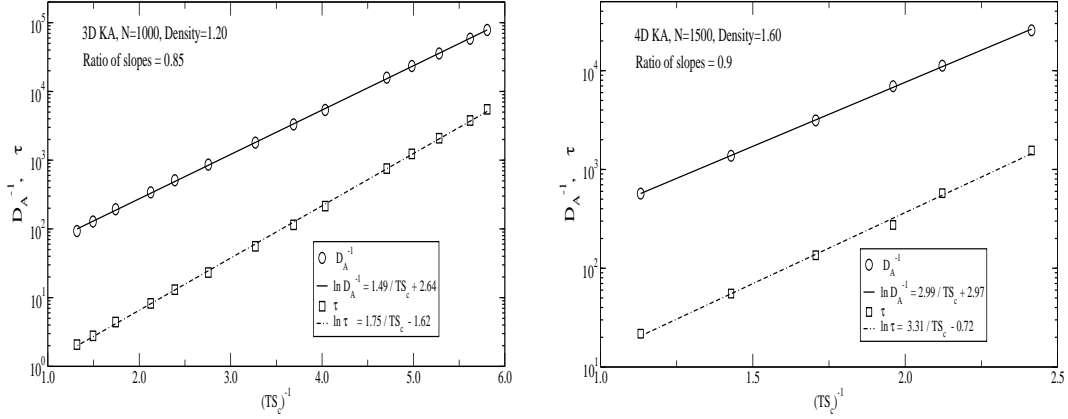
FIG. 8: *Left*: The Adam Gibbs (AG) relation in the 3DKA model using as the dynamical quantities D_A, τ. Here τ is the α relaxation time from the overlap function $q(t)$. *Right*: The AG relation in the 4DKA model using as the dynamical quantities D_A, τ. The slopes are different for D_A and τ indicating that the diffusion coefficient has a *different* dependence on the configuration entropy than the α relaxation time. The fractional SE exponent at low T can be interpreted as the ratio of the slopes (Table I).
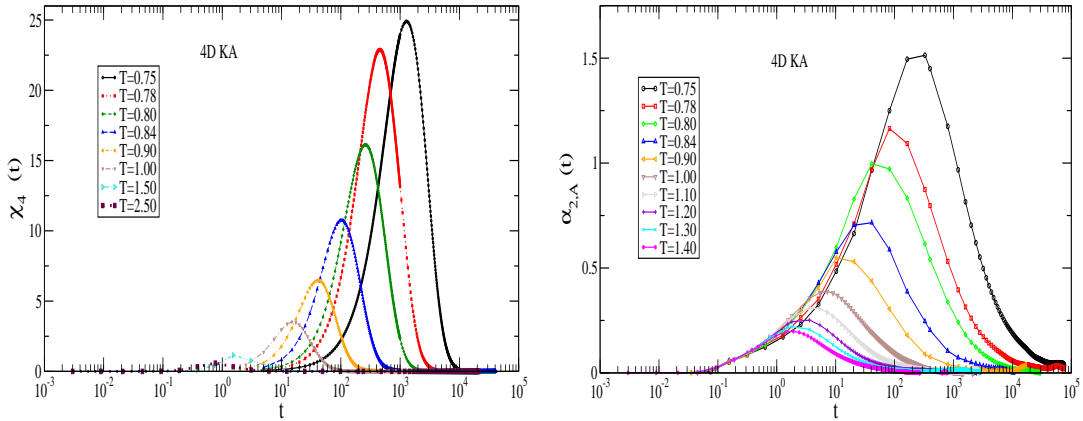

FIG. 9: The time dependences of the dynamical susceptibility $\chi_4(t)$ and of the non-Gaussian parameter $\alpha_{2,A}(t)$ in the 4DKA model. Peak values χ_4^{peak} and $\alpha_{2,A}^{peak}$ extracted from such time dependence are described further below.
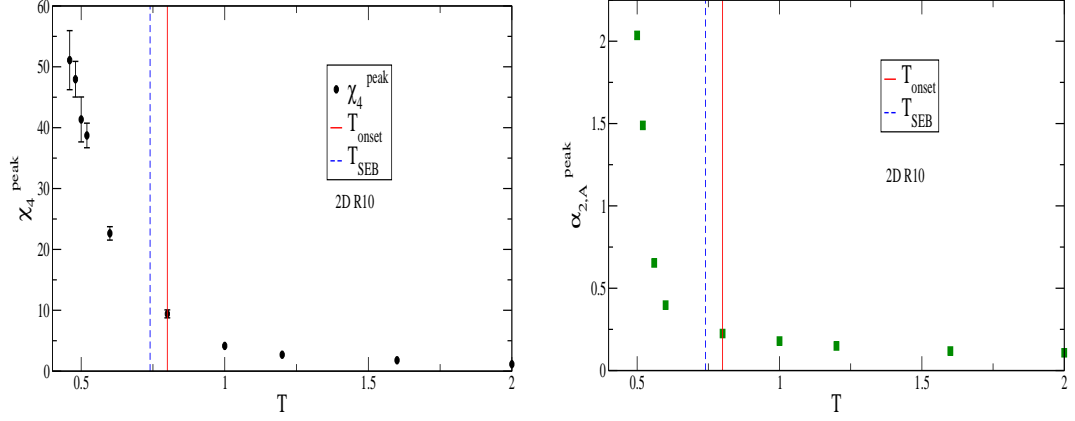
FIG. 10: *L*eft: T dependences of the peak height χ_4^{peak} of the dynamical susceptibility $\chi_4(t)$ in the 2D R10 model. *R*ight: T dependences of the peak height $\alpha_{2,A}^{peak}$ of the non-Gaussian parameter $\alpha_{2,A}(t)$ in the 2D R10 model.
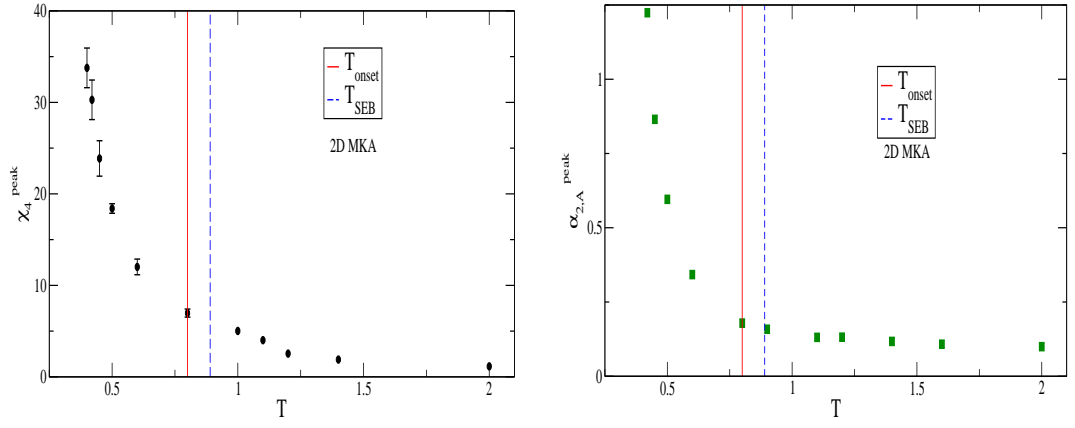

FIG. 11: *L*eft : T dependences of the peak height χ_4^{peak} of the dynamical susceptibility $\chi_4(t)$ in the 2DMKA model. *R*ight : T dependences of the peak height $\alpha_{2,A}^{peak}$ of the non-Gaussian parameter $\alpha_{2,A}(t)$ in the 2DMKA model.
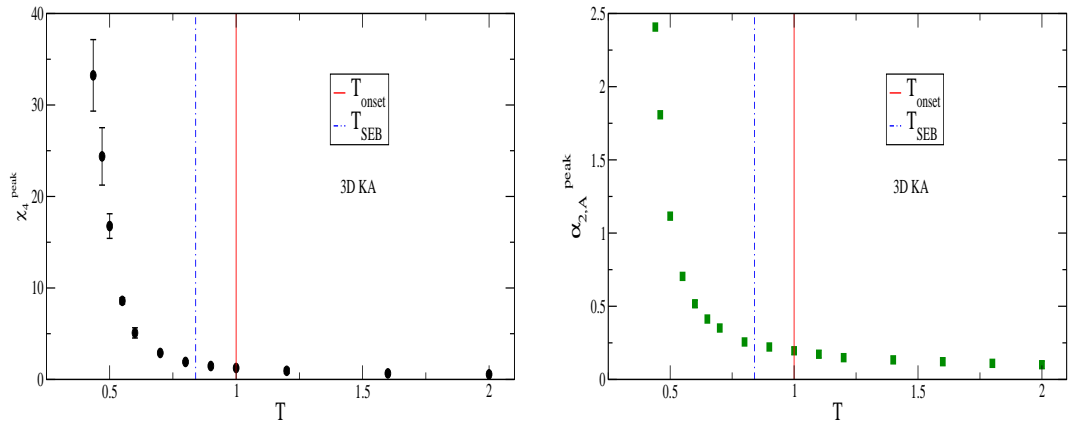

FIG. 12: *L*eft : T dependences of the peak height χ_4^{peak} of the dynamical susceptibility $\chi_4(t)$ in the 3DKA model. *R*ight : T dependences of the peak height $\alpha_{2,A}^{peak}$ of the non-Gaussian parameter $\alpha_{2,A}(t)$ in the 3DKA model.
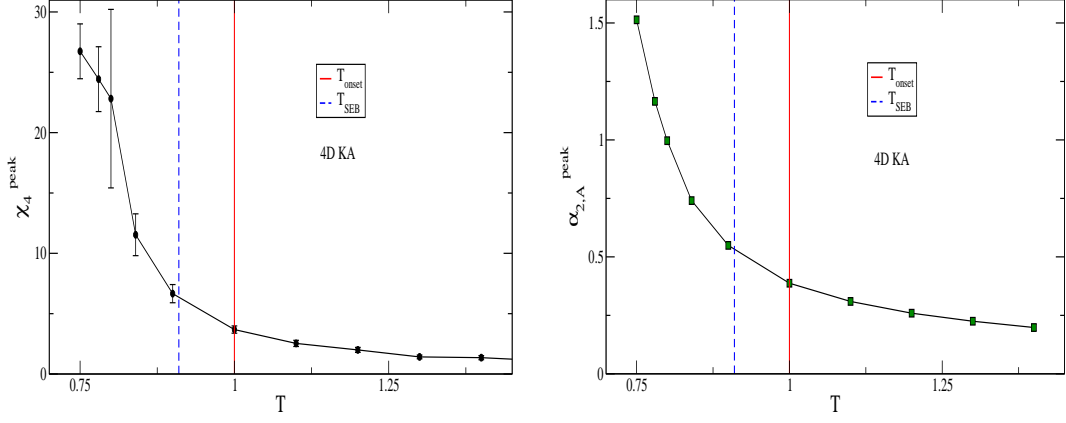
FIG. 13: *L*eft : T dependences of the peak height χ_4^{peak} of the dynamical susceptibility $\chi_4(t)$ in the 4DKA model. *R*ight : T dependences of the peak height $\alpha_{2,A}^{peak}$ of the non-Gaussian parameter $\alpha_{2,A}(t)$ in the 4DKA model.
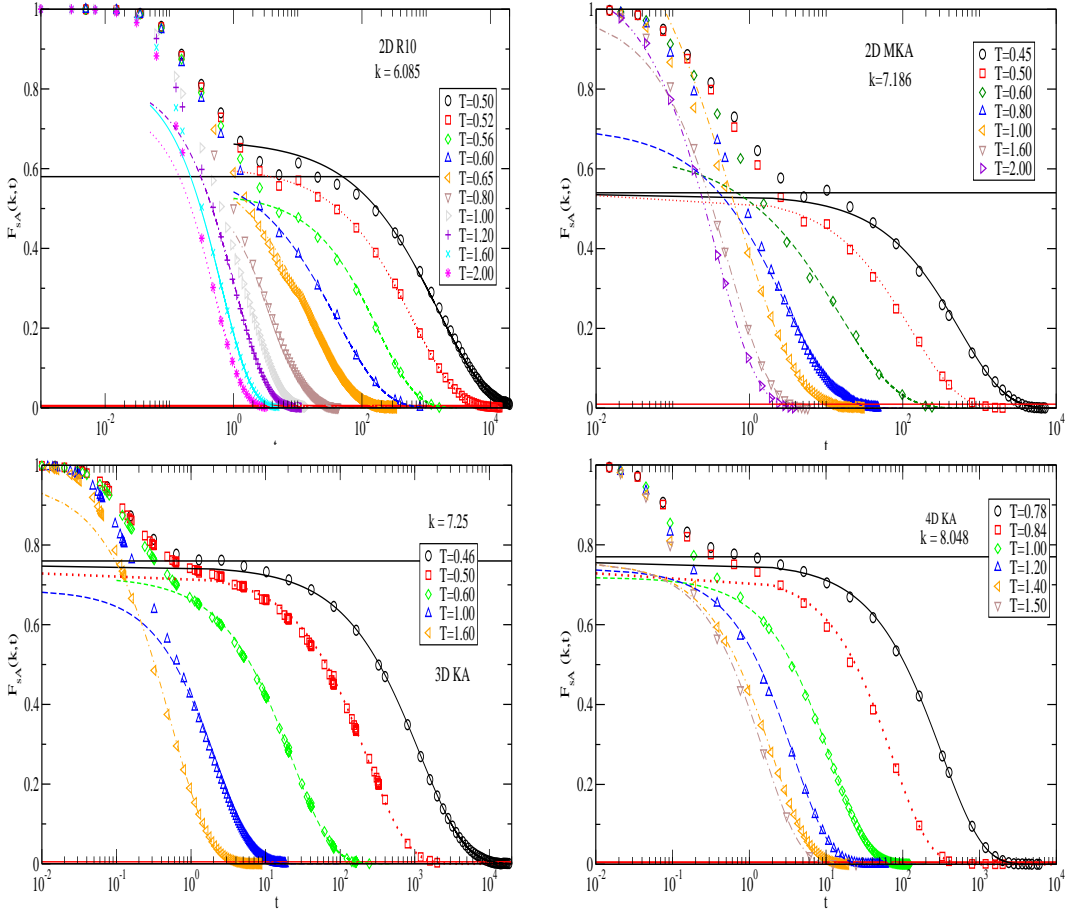

FIG. 14: T dependence of F_{sAkt} in 2DR10, 2DMKA, 3DKA and 4DKA models. Also shown are fit curves to the stretched exponential form. Horizontal lines indicate the range of y values within which the fitting is performed.

B. Dynamical heterogeneity and the breakdown of the Stokes-Einstein relation

Here we consider three measures of dynamical heterogeneity, namely the dynamical susceptibility χ_4, the non-Gaussian parameter α_2 and the stretching exponent β_{KWW}. We examine to what extent these measures of heterogeneity correlate with the degree of the breakdown of the SE relation.

Both χ_4 and α_2 have been extensively studied as indicators of dynamical heterogeneity (e. g. [37–39, 76]). These quantities are functions of time, and exhibit a maximum value at a characteristic time that is close to τ_α [39] in the case of χ_4 and to $t^* \sim (D/T)^{-1}$ in the case of α_2 [76]. The time dependence of χ_4 and α_2 are shown in Fig. 9. Peak values χ_4^{peak} and α_2^{peak} extracted from such time dependence are described further below as measures of heterogeneity.

The temperature dependence of the peak of the dynamical susceptibility χ_4^{peak} and that of the non-Gaussian parameter α_2^{peak} in different models are shown in Figs. 10, 11, 12 and 13. Clearly, in *all dimensions*, the peak heights χ_4^{peak} and α_2^{peak} grows as the temperature decreases thus indicating that the dynamics is heterogeneous in the lower part of the temperature range that we study.

As a third direct measure of the degree of dynamical heterogeneity, we estimate the stretching exponent β_{KWW}. We have computed β_{KWW} from the self intermediate scattering function F_{sAkt} for k at the peak of the structure factor. Fig. 14 shows the temperature dependence of $F_{sAkt}(k,t)$ for different models and the fits to stretched exponential form from which the stretching exponents β_{KWW} are obtained [77].

In order to compare the degree of the SE breakdown with that of dynamical heterogeneity, we plot χ_4^{peak}, $\alpha_{2,A}^{peak}$ and β_{KWW} for the different models against the relaxation time τ_α. We expect that the system showing a stronger SE breakdown at a given temperature (or relaxation time) will also show a larger degree of heterogeneity. The data in Fig. 15 for χ_4^{peak} shows that indeed, the four dimensional system by and large has smaller values of χ_4^{peak} than the three dimensional system, although the values are close especially at low temperatures. This is consistent with the larger SE breakdown observed in three dimensions. Two dimensional systems show substantially larger values of χ_4^{peak} than three dimensional systems for most of the studies points. While this is qualitatively consistent in principle with the marginal increase in the degree of SE breakdown in two dimensions, quantitatively the difference in χ_4^{peak} is large and surprising.

In similar fashion, $\alpha_{2,A}^{peak}$ values show an increase in going from four to three dimensions. However, two dimensional systems show smaller values of $\alpha_{2,A}^{peak}$ than either three or four dimensional systems. This is contrary to the relative degrees of SE breakdown in these differ-

ent systems. Such an inconsistency may reveal either a shortcoming of $\alpha_{2,A}^{peak}$ as a measure of heterogeneity, of another aspect of the peculiar behavior of two dimensional systems. Further investigations are necessary to understand this behavior.

Finally, we find that the stretching exponents β_{KWW} depend systematically on the dimensionality, even though the estiamtes are noisy. The β_{KWW} values for the four dimensional system (4DKA) lie above those of the three dimensional system (3DKA), which in turn are larger than those the values for the two dimensional systems (2DMKA and 2DR10). Though not strictly consistent with the degree of SE breakdown as quantified by the breakdown exponent, the behavior of β_{KWW} does not throw up any surprises. A more detailed study, considering also length scales over which dynamics is correlated spatially, perhaps along the lines of [71].
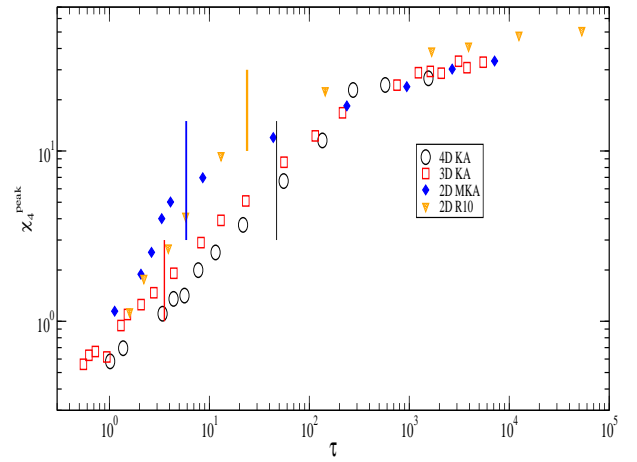

FIG. 15: Comparison of the *degree of heterogeneity in different dimensions* using the χ_4^{peak} as a measure. Vertical lines correspond to T_{SEB}

C. Dependence of the fragility on spatial dimensions

As discussed in the introduction, the fragility of a glass former has been argued to be correlated with the heterogeneity of a glass forming liquid, and by extension the degree of the breakdown of the SE relation. To evaluate such an expectation, we calculate the fragility of the model glass formers studied. We estimate the kinetic fragility from the Vogel-Fulcher-Tammann (VFT) fit to the T-dependence of the α relaxation times:

$$\tau(T) = \tau_0 \exp\left[\frac{1}{K_{VFT}(\frac{T}{T_{VFT}} - 1)}\right] \qquad (10)$$

Fig. 18 shows the T dependence of the α relaxation times in the five models we have studied, in a "fragility
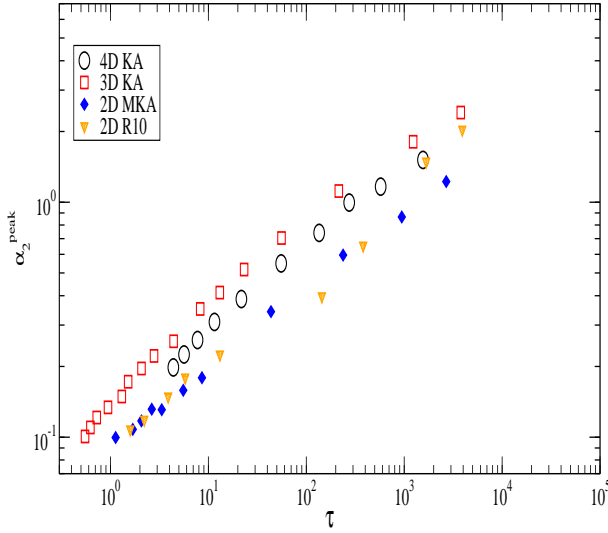
FIG. 16: Comparison of the *degree of heterogeneity in different dimensions* using $\alpha_{2,A}^{peak}$ as a measure.
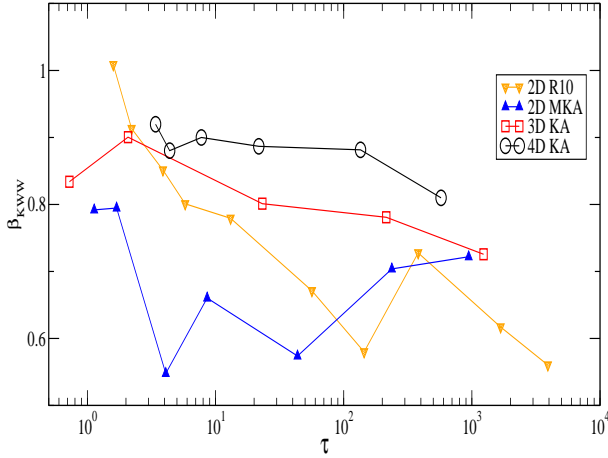

FIG. 17: Comparison of the *degree of heterogeneity in different dimensions* using the β_{KWW} as a measure.

FIG. 18: *Top:* Fragility plot of relaxation times for five models in 2,3,4 spatial dimensions. VFT fits to relaxation times shown are used to obtain the kinetic fragility K_{VFT} (see discussion). The fragility plot employs a "simulation glass transition temperature" T_g defined as $\tau(T_g) = 10^5$ (reduced unit) to scale temperatures. The K_{VFT} values are listed in Table II. *Bottom:* Fragility plot for four models in 2,3,4 spatial dimensions using the inverse of the diffusion coefficient. *The plots show that systems at higher dimensions are more fragile.*

plot" which shows relaxation times in an Arrhenius plot with the temperature scaled by the glass transition temperature. We use a "simulation glass transition temperature" T_g defined from $\tau(T_g) = 10^5$ (reduced units) in order to make such a plot. The bottom panel shows a fragility plot for the inverse diffusion coefficients, with T_g defined from $D_A^{-1} = 10^5$ (reduced units). The plots and the VFT fits to the relaxation times clearly show that the fragility of the liquids is larger at higher dimensions. This trend is opposite to the expectation based on that of the breakdown of the SE relation, and an assumption that the two are correlated. Nevertheless, there are no strong reasons to expect that fragility is correlated with heterogeneous dynamics, in particular with a variation of dimensionality. For example, the analysis by Xia
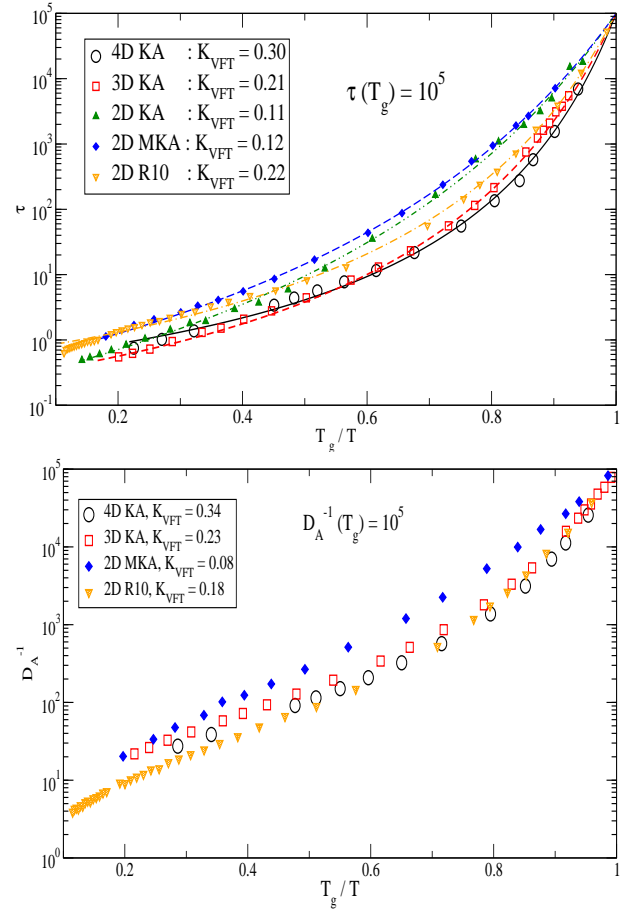
and Wolynes [43] is restricted to three dimensions, and it would be interesting to carry it out for other dimensions as well.

On the other hand, a rationalization of the fragilities themselves of the different systems studied can be attempted using the energy landscape approach in [69], based on the validity of the Adam-Gibbs relation. In order for the VFT relation and the Adam-Gibbs relation to both hold, one needs the T dependence of TS_c to be linear:

$$TS_c = K_T\left(\frac{T}{T_K} - 1\right), \qquad (11)$$
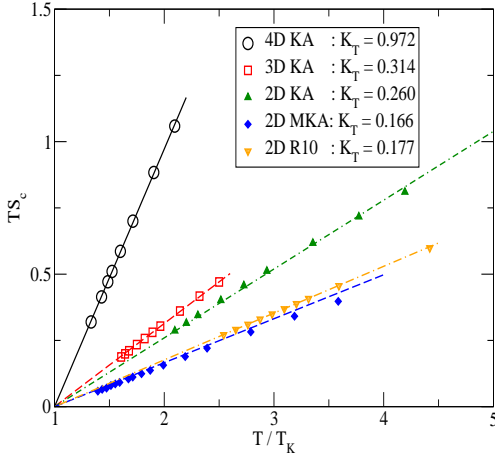
Eq. 11 defines the thermodynamic fragility K_T. The

FIG. 19: T dependence of TS_c of five models in 2,3,4 spatial dimensions plotted as TS_c *vs.* T/T_K so that the slope is an estimate of the thermodynamic fragility K_T (listed in Table II). The plot shows that the thermodynamic fragility increases with increasing spatial dimensionality.
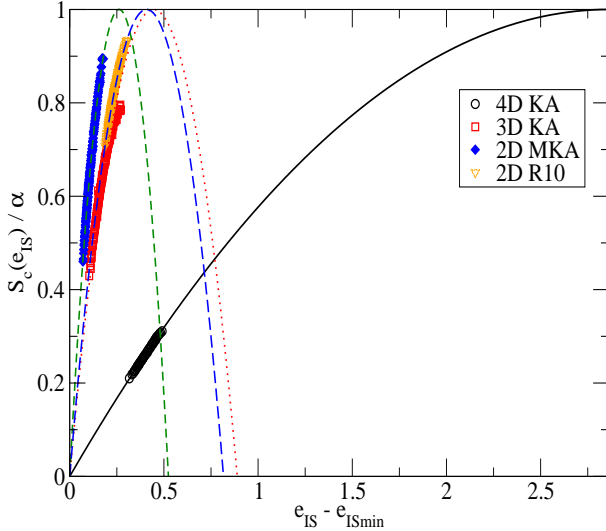

FIG. 20: The configurational entropy density $S_c(e_{IS})$ of the inherent structures plotted *vs.* their energy shifted by its minimum possible value e_{ISmin} defined from $S_c(e_{ISmin}) = 0$. The lines are fits to the parabolic form: $\frac{S_c(e_{IS})}{\alpha} = 1 - \frac{(e_{IS} - e_{IS}^0)^2}{(\sigma\sqrt{\alpha})^2}$ where $e_{IS}^0 = e_{ISmin} + \sigma\sqrt{\alpha}$ is the IS energy at the peak of the distribution. The distribution is broader for higher dimensions which partially explains the increase of the thermodynamic fragility with increasing spatial dimension.

thermodynamic fragility K_T can be related to the kinetic fragility K_{VFT} by combining the AG relation $\tau = \tau_0 \exp(\frac{A}{TS_c})$, the linear T dependence of TS_c (Eq. 11) and the VFT form (Eq. 10) to obtain [67],

$$K_{VFT} = K_T/A \qquad (12)$$

The origin of K_T can be understood from the properties of the minima of the potential energy landscape [69], known as "inherent structures" (IS). The configurational entropy is the entropy associated with the multiplicity of energy minima, and if the density of states of such minima with respect to their energy e_{IS} is described by

$$S_c(e_{IS})/Nk_B = \alpha - \frac{(e_{IS} - e_{IS}^0)^2}{\sigma^2} \qquad (13)$$

such that α quantifies the total number of inherent structures, and σ^2 the variance of the distribution, the thermodynamic fragility (under the simplifying assumption of the vibrational entropies of all the inherent structures being the same) is given by

$$K_T = \sqrt{\alpha}\sigma/2. \qquad (14)$$

In other words, K_T is proportional to the total spread of the density of states. Fig. 19 shows the T dependence of the configurational entropy for five models. We see that the thermodynamic fragility increases significantly as the spatial dimension increases. Further, in Fig. 20 we show that the quantity $\sigma\sqrt{\alpha}$ estimating the width of the configurational entropy density increases with increasing spatial dimension, which partially explains the increase of the thermodynamic fragility with increasing spatial dimensions.

Eq. 12 formally resolves the contributions of configurational entropy (K_T) and the energy barrier (A) to the kinetic fragility. Figs. 19 and 20 shows that the configurational entropy contribution increases with increasing dimension thus by itself explaining the increase in the kinetic fragility at higher dimensions. The characteristic parameters related to fragility for the five models studied here are summarized in Table II.

V. SUMMARY AND CONCLUSIONS

In this work we have attempted to analyze the breakdown of the Stokes-Einstein relation in systems of spatial dimensionality 2, 3 and 4, and its relation to the thermodynamics of the system in the form of the variation of configurational entropy, and various aspects of dynamical heterogeneity. We summarize here the salient findings of this work: (i) We find that in systems in all spatial dimensions, the low temperature relationship between diffusion and structural relaxation times is well described by a fractional Stokes-Einstein relationship. (ii) The high temperature behavior is consistent with the Stokes-Einstein relationship in four and three dimensions, but we find that in the two dimensional systems we study, the SE relation is not valid at high temperatures also. In particular, representing the behavior as a fractional SE relationship, we find the exponent to be bigger than 1. (iii) We find that the observed breakdown at low temperatures can be rationalized and understood in terms of

the different activation free energies for diffusion and relaxation times in three and four dimensions, and in terms of a generalized Adam-Gibbs relation in two dimensions. (iv) We find that the crossover from high temperature to low temperature behavior (which constitutes a breakdown of the SE relation for three and four dimensional systems) occurs close to the onset temperature of slow dynamics, rather than close to the mode coupling temperature as previously discussed. (v) We find that the exponent characterizing the SE breakdown is different for different systems even for the same spatial dimensions (as seen in two and three dimensions) calling into question theories which claim universal exponents for a given spatial dimension. (vi) We find that the degree of breakdown of the SE relation correlates reasonably well with measures of dynamical heterogeneity, but with notable exceptions such as the temperature dependence of the non-Gaussian parameter α_2. (vii) We find that the dependence of fragility on spatial dimensionality is the opposite of the degree of the breakdown of the SE relation, with fragility becoming larger in higher spatial dimensions. Although surprising, a strong case for a correlation between fragility and heterogeneity is not a given, and arguments for such a correlation in three dimensions need to be examined in light of our results for their applicability to other dimensions. It would be interesting to pursue some of the questions raised by our work in higher spatial dimensions as well, such as recently done in attempting to identify an upper critical dimension [78], which will hopefully clarify some of the open questions.

[1] J. Hansen and I. R. McDonald, Theory of Simple Liquids (3rd Ed.), Elsevier (2008).

[2] A. Einstein, Ann. Phys. **17**, 549 (1905); English translation: A. Einstein, Investigations on the theory of the Brownian movement, Dover, NY (1956).

[3] L. D. Landau and E. M. Lifshitz, Fluid Mechanics, 2nd. Ed., Pergamon Press (1987).

[4] J. A. Hodgdon and F. H. Stillinger, *Phys. Rev. E*, **48**, 207 (1993); F. H. Stillinger and J. A. Hodgdon, *Phys. Rev. E*, **50**, 2064 (1994).

[5] G. L. Pollack, *Phys. Rev. A*, **23**, 2660 (1981).

[6] F. Fujara, B. Geil, H. Sillescu and G. Fleischer, *Z. Phys. B*, **88**, 195 (1992); I. Chang, F. Fujara, B. Geil, G. Heuberger, T. Mangel and H. Silescu, *J. Non-Cryst. Solids*, **172-174**, 248 (1994).

[7] I. Chang and H. Silescu, *J. Phys. Chem. B*, **101**, 8794 (1997).

[8] G. Heuberger and H. Sillescu, *J. Phys. Chem.*, **100**, 15255 (1996).

[9] M. T. Cicerone and M. D. Ediger, *J. Chem. Phys.*, **104**, 7210 (1996); M. T. Cicerone, F. R. Blackburn, and M. D. Ediger, *ibid.*, **102**, 471 (1995).

[10] F. R. Blackburn, C. Yang and M. D. Ediger, *J. Phys. Chem.*, **100**, 18249 (1996).

[11] M. K. Mapes, S. F. Swallen, K. L. Kearns and M. D. Ediger, *J. Chem. Phys.*, **124**, 054710 (2006).

[12] S. F. Swallen, K. Traynor, R. J. McMahon, M. D. Ediger and T. E. Mates, *J. Phys. Chem. B*, **113**, 4600 (2009).

[13] S. F. Swallen, P. A. Bonvallet, R. J. McMahon and M. D. Ediger, *Phys. Rev. Lett.*, **90**, 015901 (2003).

[14] E. Rössler, Phys. Rev. Lett., **65**, 1595, (1990); E. Rössler and P Eiermann, J. Chem. Phys., **100**, 5237 (1994).

[15] S. S. Ashwin, Ph D. Thesis (2005).

[16] W. Kob and H. C. Andersen, Phys. Rev. Lett., **73**, 1376 (1994).

[17] G. Tarjus and D. Kivelson, J. Chem. Phys., **103**, 3071 (1995).

[18] G. Monaco, D. Fioretto, L. Comez and G. Ruocco, Phys. Rev. E, **63**, 061502, (2001).

[19] K. Ngai, J. Magill and D. Plazek, *J. Chem. Phys.*, **112**, 1887 (1999).

[20] C. Hansen, F. Stickel, T. Berger, R. Richert, and E. W. Fischer, *J. Chem. Phys.*, **107**, 1086 (1997).

[21] L. Liu *et al.*, *Phys. Rev. Lett.*, **95**, 117802 (2005).

[22] S. Chen *et al.*, *Proc. Natl. Acad. Sci. (US)*, **103**, 12974 (2006).

[23] S. Becker, P. Poole, F. Starr, *Phys. Rev. Lett.*, **97**, 055901, (2006).

[24] F. Fernandez-Alonso, F. J. Bermejo, S. E. McLain, J. F. C. Turner, J. J. Molaison, and K. W. Herwig, *Phys. Rev. Lett.*, **98**, 077801 (2007).

[25] F. Mallamace *et al.*, *J. Phys. Chem. B*, **114**, 1870, (2010).

[26] L. Xu *et al.*, *Nature Physics*, **5**, 565, (2009).

[27] M. D. Ediger, *Annu. Rev. Phys. Chem.* **51**, 99 (2000).

[28] C. De Michele and D. Leporini, *Phys. Rev. E* **63** 036701 (2001).

[29] Bordat *et al.*, *J. Phys.: Condens. Matter*, **15**, 5397 (2003).

[30] F. Affouard, M. Descamps, L.-C. Valdes, J. Habasaki, P. Bordat, and K. L. Ngai, *J. Chem. Phys.*, **131**, 104510 (2009).

[31] X. J. Han and H. R. Schober, *Phys. Rev. B*, **83**, 224201 (2011).

[32] S. Sastry, P.G. Debenedetti and F. H. Stillinger, Nature, **393**, 554 (1998).

[33] S. Sastry, *PhysChemComm*, **14**, (2000).

[34] S. Sastry *et. al. Physica A* **270** 301 (1999).

[35] T. R. Kirkpatrick and D. Thlrumalal, *Phys. Rev. A*, **37**, 4439 (1988).

[36] C. Dasgupta, A. V. Indrani, S. Ramaswamy and M. K. Phani, *Europhys. Lett.* **15**, 307 (1991).

[37] S. C. Glotzer, V. N. Novikov and T. B. Schrøder, *J. Chem. Phys.* **112**, 509 (2000).

[38] C. Donati *et al.*, *J Non-Cryst Solids*, **307**, 215224 (2002).

[39] S. Karmakar, C. Dasgupta, S. Sastry, *Proc. Natl. Acad. Sci. (US)* **106**, 3675, (2009).

[40] L. Berthier, G. Biroli, J-P. Bouchaud and R. L. Jack, Chapter of "Dynamical heterogeneities in glasses, colloids, and granular media", Eds.: L. Berthier, G. Biroli, J-P Bouchaud, L. Cipelletti and W. van Saarloos (Oxford Univ. Press, 2011); *arXiv:1009.4765v2 [cond-mat.stat-mech]*, (2010).

[41] Y. Jung,1 J. P. Garrahan and D. Chandler, *Phys. Rev. E*, **69**, 061205 (2004); J. Chem. Phys. **123** 084509 (2005)..

[42] X. Xia and P. G. Wolynes, *J. Phys. Chem. B* **105**, 6570 (2001).

[43] X. Xia and P. G. Wolynes, *Phys. Rev. Lett.* **86**, 65526 (2001).

[44] V. Lubchemko and P.G. Wolynes, Ann. Rev. Phys. Chem. **58**, 235 (2007).

[45] G. Biroli and J.P. Bouchaud, J. Phys. Cond. Mat, **19**, 205101 (2007).

[46] J. S. Langer, arXiv:1108.2738v2 [cond-mat.stat-mech] (2011).

[47] J.F. Douglas and D. Leporini, *J. Non-Cryst. Solids*, **235**, 137 (1998).

[48] E. La Nave, S. Sastry and F. Sciortino, *Phys. Rev. E*, **74**, 050501(R) (2006).

[49] W. Kob, H. C. Andersen, *Phys. Rev. E*, **51**, 4626 (1995).

[50] F. Alvarez, A. Alegria and J. Colmenero, *Phys. Rev. B*, **44**, 7306 (1991).

[51] R. Böhmer, K. L. Ngai, C. A. Angell and D. J. Plazek, *J. Chem. Phys.* **99**, 4201 (1993);

[52] K. Niss, C. Dalle-Ferrier, G. Tarjus, C. Alba-Simionesco, *arXiv:cond-mat/0611253v1 [cond-mat.soft]*, (2006).

[53] A. Heuer, *J. Phys.: Condens. Matter*, **20**, 373101 (2008).

[54] J. C. Dyre, *J. Phys. Condens. Matt.*, **19**, 205105 (2007).

[55] V. V. Vasisht and S. Sastry (manuscript in preparation).

[56] M. H. Ernst, E. H. Hauge, and J. M. J. Van Leeuwen, Phys.Rev. Lett. **25**,1254 (1970).

[57] J. R. Dorfman and E. G. D. Cohen, Phys. Rev. Lett. **25**, 1257 (1970).

[58] J. F. Douglas, Comp. Material Science vol. **4**, 292 (1995).

[59] B. Liu and J. Goree, Phys. Rev. Lett. **94**, 185002 (2005).

[60] B. Liu, J. Goree and O.S. Vaulina, Phys. Rev. Lett. **96**, 015005 (2006).

[61] D. Gravina, G. Ciccotti, and B. L. Holian, Phys. Rev. E **52**, 6123 (1995).

[62] W. G. Hoover and H. A. Posch, Phys. Rev. E **51**, 273 (1995).

[63] R. Bruning *et al.*, J. Phys.: Condens. Matter , **21**, 035117 (2009).

[64] Karmakar et. al., Phys. Rev. Lett., **104**, 215502 (2010).

[65] D. Brown and J. H. R. Clarke, *Mol. Phys.*, **51**, 5, 1243 (1984).

[66] N. Lačević, F. W. Starr, T. B. Schrøder, and S. C. Glotzer, *J. Chem. Phys.* **119**, 7372 (2003).

[67] S. Sengupta, F. Vasconcelos, F. Affouard, and S. Sastry, *J. Chem. Phys.* **135**, 194503 (2011).

[68] S. Sengupta *et. al. Phys. Rev. Lett.* **109** 095705 (2012).

[69] S. Sastry, *Nature*, **409**, 164 (2001).

[70] F. Mezei *et. al. Phys. Rev. Lett.* **58**, 571, (1987).

[71] S-H. Chong and W. Kob, *Phys. Rev. Lett.* **102**, 025702, (2009).

[72] R. Yamamoto and A. Onuki, *Phys. Rev. Lett.* **81**, 4915 (1997).

[73] J. D. Eaves and D. R. Reichmann, *Proc. Natl. Acad. Sci. (US)* **106**, 15171, (2009).

[74] P. Charbonneau, A. Ikeda, J. A. van Meel, and K. Miyazaki, *Phys. Rev. E*, **81**, 040501 (R), (2010).

[75] D. N. Perera and P. Harrowell, *Phys. Rev. Lett.*, **81**, 120, (1998).

[76] F. W. Starr, J. F. Douglas and S. Sastry, submitted to *J. Chem. Phys.*, (2012).

[77] In order to obtain estimates of β_{KWW}, we fit the functions $F_s(k,t)$ to the stretched exponential form $F_s(k,t) = f_c \exp(-(t/\tau)^{\beta_{KWW}})$. In order to remove the influence of the short time decay of $F_s(k,t)$ on the one hand, and the noisy long time data on the other, we fit the $F_s(k,t)$ from the plateau value at the lowest temperature, down to a lower cutoff in the range $0.001 - 0.005$.

[78] P. Charbonneau, G. Parisi and F. Zamponi, http://arxiv.org/abs/1210.6073

TABLE II: Fragility-related parameters for the models in different dimensions. T_K is the Kauzmann temperature obtained from extrapolating TS_c to zero. K_{VFT} is the kinetic fragility obtained from VFT fits to relaxation times. K_T is the thermodynamic fragility obtained from the T-dependence of TSc. A is the Adam-Gibbs coefficient. $K_{AG} = K_T/A$ is the kinetic fragility estimated from the AG relation.

Model	Density	T_K	T_{VFT}	T_g	K_{VFT}	K_T	A	$K_{AG} = K_T/A$
4D KA	1.60	0.525	0.530	0.676	0.30	0.972	3.382	0.29
3D KA	1.20	0.28	0.295	0.402	0.21	0.314	1.79	0.17
2D KA	1.20	0.477	0.501	0.852	0.11	0.260	-	-
2D MKA	1.20	0.251	0.214	0.361	0.12	0.166	-	-
2D R10	0.85	0.181	0.326	0.453	0.22	0.177	-	-